The solid state phase transition of gallium particles and its size dependence

2009 J. Phys.: Condens. Matter 21 245403

(http://iopscience.iop.org/0953-8984/21/24/245403)

J. Phys.: Condens. Matter **21** (2009) 245403 (5pp) doi:10.1088/0953-8984/21/24/245403

The solid state phase transition of gallium particles and its size dependence

Xiao Meng Chen, Guang Tao Fei[1] and Kang Zheng

Key Laboratory of Materials Physics and Anhui Key Laboratory of Nanomaterials and Nanotechnology, Institute of Solid State Physics, Hefei Institutes of Physical Science, Chinese Academy of Sciences, PO Box 1129, Hefei 230031, People's Republic of China

E-mail: gtfei@issp.ac.cn

Received 20 March 2009, in final form 28 April 2009
Published 21 May 2009
Online at stacks.iop.org/JPhysCM/21/245403

Abstract

Submicrometer-sized Ga particles were dispersed in polymethylmethacrylate (PMMA) matrix by an ultrasonic vibration and sedimentation method. The solid phase transition from γ-Ga to δ-Ga and its Ga particle size dependence were studied by means of differential scanning calorimeter measurements. It was shown that a solid–solid phase transition corresponding to the γ-Ga $\rightarrow$ δ-Ga one happened in Ga particles upon cooling. Moreover, the ratio of the particles undergoing the solid phase transition to all particles increases with decrease of the particle size.

1. Introduction

Ga is a peculiar metal which has many stable and metastable phases. The physical properties of Ga have been studied extensively in the past few decades [1–6]. Although great effort has focused on the undercooling property [7, 8], confined geometry effect [9–11], size effect [12, 13] and new phase structures of fine Ga particles [14–16], the formation process and formation mechanism for metastable Ga phases are still unclear. In these previous studies, it was shown that metastable Ga phase structures were crystallized directly from the undercooled liquid metal in a cooling process and the metastable Ga melt changed to the liquid in a heating process [17–19]. Recently, Di Cicco *et al* [20] have found solid–solid phase transitions of Ga particles embedded in epoxy resin by means of energy-dispersive x-ray diffraction (EDXRD) and x-ray absorption fine structure (XAFS), in a warming process. However, no solid phase transitions of Ga have been reported in cooling processes. In this paper, we study the solid–solid phase transition of fine Ga particles confined in PMMA matrix in a cooling process by using a differential scanning calorimeter (DSC) method. The aim of the present paper is to study the peculiar phase transition processes in fine Ga particles.

[1] Author to whom any correspondence should be addressed.

2. Experiments

Ga particles dispersed in PMMA matrix were prepared according to the method described previously [12]. The procedures of sample preparation were as follows: firstly, methylmethacrylate (MMA) monomer was rinsed with 5 wt% of caustic soda solution in a delivery flask until the color of the MMA became achromatic, in order to remove the inhibitor (hydroquinone). Then the solution was rinsed with distilled water to make it neutral, and this was followed by desiccating with anhydrous sodium sulfate. Secondly, ultrasonic vibration was used to fragment and disperse Ga (purity: 99.9999%) into the MMA monomer liquid. The mass proportion of the metal to the mixture was set at 20%. Thirdly, dibenzoyl peroxide was added to accelerate the polymerization. The liquid mixture was injected into an $80 \times 50 \times 3$ mm^3 glass mold and annealed in the air. The temperature was set at 60 °C for 2 h and then 80 °C for 1 h. Finally, after removing the mold, solid PMMA with well-dispersed Ga droplets was obtained. Unlike Ga particles in other matrices such as porous glass and opal, the Ga particles in the PMMA matrix are isolated from each other.

These Ga/PMMA composites were sliced at different distance (D) from the bottom of the same sample. Figure 1 is a schematic diagram of the Ga/PMMA composites and the sampling position (D). The particle size was measured using a JEM-100SX transmission electron microscope (TEM). The specimen for TEM observation was made using an ultramicrotome, and the thickness of the specimen is about 70 nm. In order to obtain statistics for the droplet size

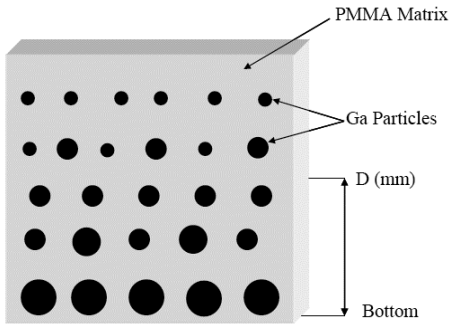

Figure 1. Schematic diagram of the Ga/PMMA composites and the sampling position (D).

distribution, 400 particles for each sample were counted in our experiment.

The differential scanning calorimeter (DSC) experiments were carried out with Perkin-Elmer Pyris Diamond DSC equipment. The DSC measurement procedures for each sample were carried out in the temperature range from 50 to −160 °C. Cooling was performed using liquid nitrogen with a cooling scanning rate of 20 °C min^{-1}. Then the sample was heated with a heating scanning rate of 5 °C min^{-1}. During the DSC measurements, helium gas was introduced into the sample chamber in order to prevent the liquid nitrogen from freezing. The amount of each specimen loaded in the aluminum pan for DSC measurement was about 10 mg, and the thickness of the DSC specimens is about 0.2 mm.

3. Results and discussion

Solid PMMA with well-dispersed Ga droplets was obtained by procedures of ultrasonic vibration and sedimentation. Due to the great difference in the specific gravity ρ between Ga and MMA, Ga droplets with bigger diameter sediment more quickly than the smaller ones. Moreover, in order to reduce the surface energy, those droplets that have reached the bottom may have a high aggregate possibility of becoming bigger ones. Detailed explanation can be found in our recent report [13]. And the TEM observation confirmed that Ga particles are distributed in PMMA matrix with a size gradient.

Figure 2 is a representative TEM picture of Ga/PMMA composite; it shows that the spherical Ga droplets with different sizes are well separated in PMMA. Figure 3 is the particle size distribution histogram for different samples. It can be seen that the average particle size gradually shifts toward smaller size from sample 1 to sample 2 and sample 3. The average sizes of the particles obtained at the positions $D = 0$ (sample 1), 3 (sample 2), 30 mm (sample 3), were about 0.51, 0.44 and 0.31 μm, respectively. The average size is hereafter taken as the size of the particles in the matrix.

Figures 4(a)–(f) is the DSC heating trace for sample 2, which was heated after cooling down to −160 °C, −140 °C, −130 °C, −120 °C, −100 °C, and −80 °C, respectively. In figures 4(a)–(d), three endothermal peaks with the onset temperature located at −33.7, −17.7 and −14.7 °C were detected. And there was no evident endothermal peak

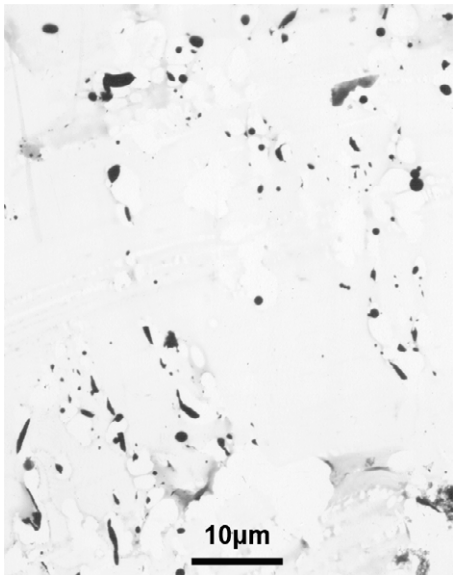

Figure 2. TEM image of Ga particles dispersed in PMMA at position $D = 3$ mm (sample 2). The distance from the bottom of the Ga/PMMA composite samples was defined as D.

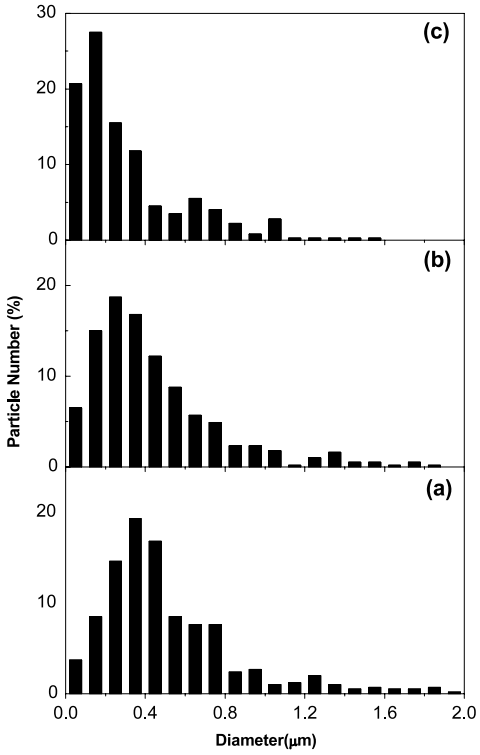

Figure 3. Particle size distribution histograms for Ga particles in PMMA matrix determined from the TEM images of different samples corresponding to $D = 0$ mm (a), 3 mm (b), and 30 mm (c), respectively.

within the temperature range from −160 to −50 °C. These three peaks can be related to the melting processes of γ-Ga (−35.6 °C), δ-Ga (−19.4 °C) and β-Ga (−16.2 °C), respectively [12, 17]. However, the onset temperature of each peak is about 2 °C higher than the melting temperatures

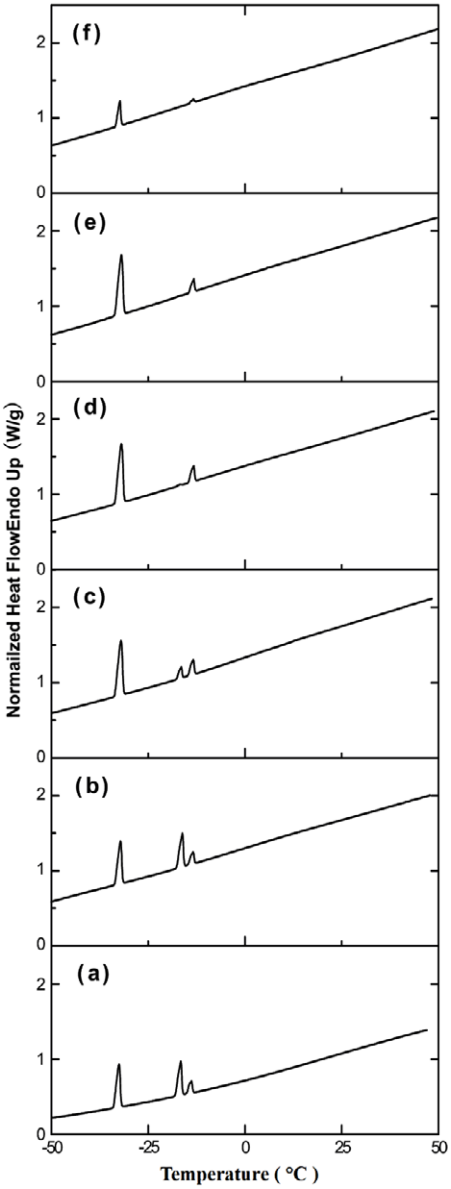

Figure 4. DSC heating traces for sample 2 after cooling down to particular temperatures. (a), (b), (c), (d), (e) and (f) are the DSC traces with the starting heating temperature −160 °C, −140 °C, −130 °C, −120 °C, −100 °C, and −80 °C, respectively.

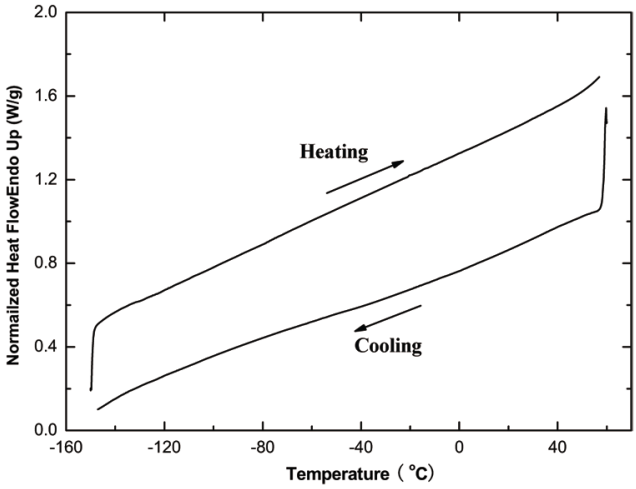

Figure 5. DSC heating and cooling curves for pure PMMA matrix.

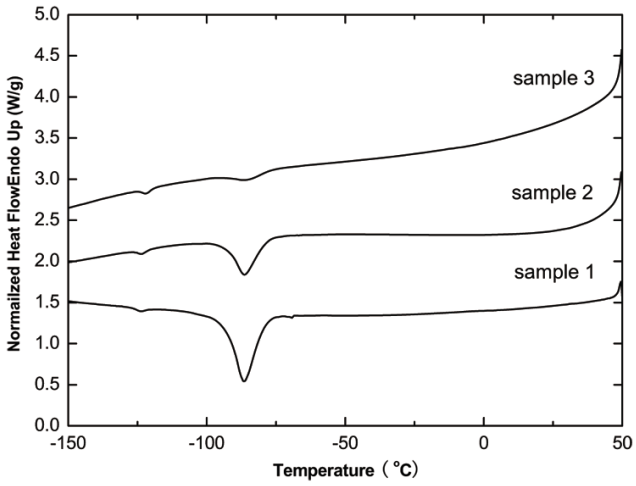

Figure 6. DSC cooling traces for sample 1, sample 2 and sample 3.

from the literature [21], which might be due to the poor heat conduction of the PMMA matrix. It can be found that only two endothermal peaks with the onset temperature located at −33.7 and −14.7 °C were observed in figures 4(e) and (f). This means the δ-Ga can only appear when the sample is cooled down to below −120 °C.

For comparison, the DSC heating and cooling curves for pure PMMA matrix were also obtained. Figure 5 shows that there was no evident peak within the temperature range from −150 to 60 °C for pure PMMA. This indicates that the peaks which have been observed in both DSC heating and cooling curves in Ga/PMMA composites were caused by the Ga particles, not by the PMMA matrix.

Figure 6 shows the DSC cooling traces for three samples. The samples were cooled down from 50 to −160 °C with a cooling rate of 20 °C min^{-1}. There are two broadened exothermic peaks with the onset temperatures of −80 and −120 °C. Comparing with figure 4, it can be found that the exothermic peaks located at −80 °C can be attributed to the freezing transition of γ-Ga and β-Ga. And the −80 °C exothermic peaks decrease with decrease of the particle size. However, the peak at −120 °C had not been reported before. We consider that this exothermic peak may correspond to a solid–solid phase transition of γ-Ga $\rightarrow$ δ-Ga, which can be seen clearly in figure 7.

Figure 7 shows the starting heating temperature dependence of the areas under the endothermal peaks for the various phases of Ga particles in DSC heating measurements. The X-axis gives the starting heating temperatures of the samples which had already cooled down; the Y-axis gives the normalized endothermal peak area which represents the mass for the various phases. All points on the curves are obtained from a series of DSC heating traces. As can be seen, the curves for the three samples have similar change tendencies for β-Ga, γ-Ga and δ-Ga phases. For sample 1, the endothermal peaks of α-Ga can also be found; however, this peak is very small,

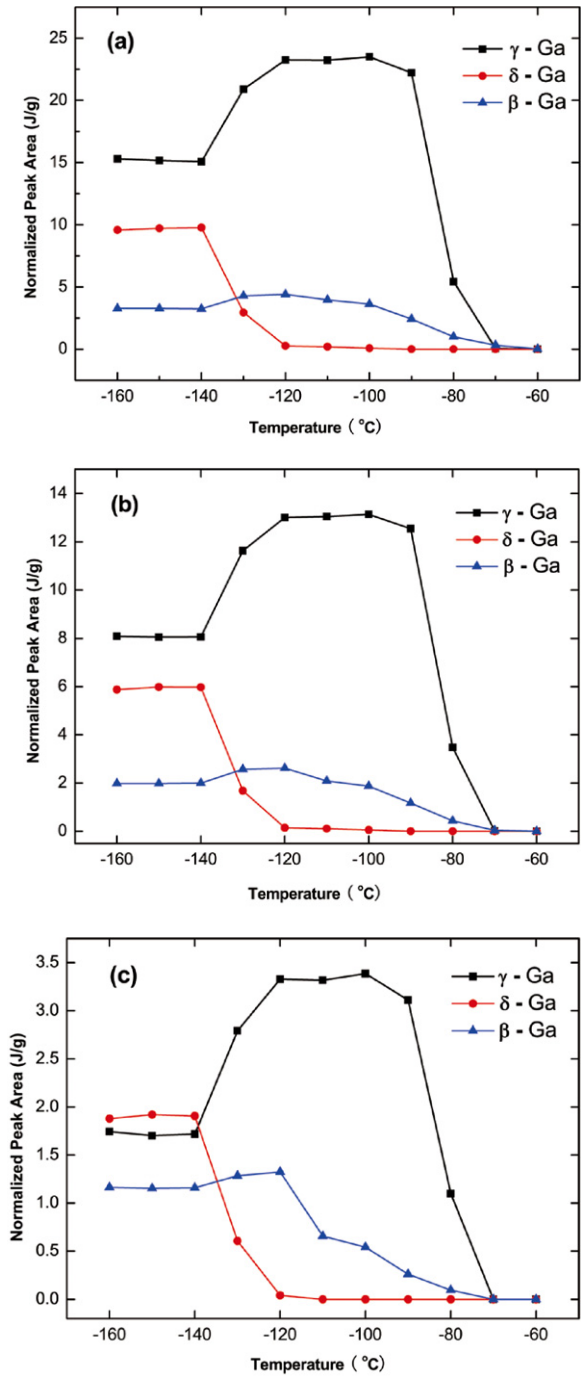

Figure 7. The starting heating temperature dependence of the areas under the endothermal peaks of the various phases of Ga particles in DSC heating measurements. The X-axis gives the starting temperature of the DSC heating measurement, and the Y-axis gives the normalized endothermal peak area acquired from the DSC heating curve. (a), (b) and (c) correspond to sample 1, sample 2, and sample 3, respectively.

(This figure is in colour only in the electronic version)

so we do not shown it in figure 7(a). When the samples were cooled below −80 °C both γ-Ga and β-Ga phases appeared. For γ-Ga, the peak area rapidly increases to a maximum at about −100 °C with temperature decrease, and remains almost unchanged until the obvious decrease at −120 °C occurs. Meanwhile, within the temperature range from −120 to −140 °C, the δ-Ga peak appears and its area rapidly reaches a maximum. This temperature range corresponds to the exothermic peak with the onset temperature at −120 °C. According to the analysis above, it can be concluded that there is a solid phase transition of γ-Ga to δ-Ga at −120 °C. For β-Ga, the peak area slightly increases on cooling down to low temperatures and reaches a maximum at −120 °C. Since a portion of β-Ga disappears within the temperature range from −120 to −140 °C, this might be assigned to a solid phase transition too.

Table 1. Areas under the γ-Ga endothermal peaks at −120 and −140 °C determined using DSC.

	Size (μm)	$A_{\gamma-120\,^\circ\mathrm{C}}$ (J g^{-1})	$A_{\gamma-140\,^\circ\mathrm{C}}$ (J g^{-1})	ΔA_γ (%)
Sample 1	0.51	23.26	15.07	35.2
Sample 2	0.44	13.05	8.05	38.3
Sample 3	0.31	3.33	1.72	48.3

Table 1 lists the γ-Ga peak areas at −120 and −140 °C for three samples. A_γ is the normalized area under the endothermal peak of γ-Ga. Here we use the following equation:

$$\Delta A_\gamma = \frac{A_{\gamma,-120\,^\circ\mathrm{C}} - A_{\gamma,-140\,^\circ\mathrm{C}}}{A_{\gamma,-120\,^\circ\mathrm{C}}} \times 100\% \qquad (1)$$

to evaluate ΔA_γ, which represents the amount of γ-Ga undergoing the solid phase transition. For samples 1, 2 and 3, ΔA_γ is 35.2%, 38.3% and 48.3%, respectively. It can be seen that the ratio of the solid phase transition from γ-Ga to δ-Ga increases with decreasing particle size. The DSC cooling traces of the three samples in figure 6 confirm the presence of the size-dependent solid phase transition phenomena too. That is because the areas of the two exothermic peaks can be used to evaluate the mass of the Ga particles undergoing the liquid–solid (with the onset temperature at −80 °C) and solid–solid (with the onset temperature at −120 °C) phase transitions. In figure 6 it is clear that, after the complete freezing of Ga liquid droplets at −120 °C, solid particles in sample 3 are more favorably transformed to δ-Ga phase than ones in sample 1. This behavior indicates there is a size effect on the solid phase transition for Ga particles.

In our experiment, the phase transition of γ-Ga to δ-Ga is a first-order phase transition, so it should be governed by kinetic effects such as nucleation and growth. As we know, undercooling is a very important factor in the nucleation process. When the particles of γ-Ga phase are cooled down to the transition temperature at −120 °C, it transforms to δ-Ga phase, which might be more stable at lower temperature. The size effect on the solid phase transition might have two reasons. On the one hand, since the specific area and surface energy are inversely proportional to the size of the droplets, particles of different sizes might have different driving forces for solid phase transitions, which determine the phase transitions in nucleation and crystal growth processes. On the other hand, the confined geometry effect of the PMMA matrix should also be taken into account. In our experiment, except for a small amount of α-Ga phase being found in sample 1, the stable

phase α-Ga in ambient conditions was absent from samples 2 and 3. Since Ga is a water-like element, it expands when frozen into a α-Ga phase structure [20]. Perhaps pores with different sizes in PMMA matrix have different influences in the solid phase transition process. As the phase structures of Ga are more complicated than those of most metals, further investigations on the phase transitions are needed.

4. Conclusion

In summary, the solid–solid phase transition from γ-Ga to δ-Ga for fine Ga particles confined in PMMA matrix was first observed when cooling down to below $-120\,^{\circ}$C from DSC measurements. Moreover, the solid phase transition shows size-dependent phenomena. It is found that the ratio of the particles undergoing the solid phase transition to all particles increases with decrease of the particle size.

Acknowledgments

This work was supported by the National Natural Science Foundation of China (Nos 50671099, 50172048, 10374090 and 10274085), Ministry of Science and Technology of China (No. 2005CB623603), and Hundred Talent Program of the Chinese Academy of Sciences.

References

[1] Turnbull D and Cech R E 1950 *J. Appl. Phys.* **21** 804
[2] Bosio L, Defrain A and Dupont M 1971 *J. Chim. Phys. Phys.-Chim. Biol.* **68** 542
[3] Bosio L and Windsor C G 1975 *Phys. Rev. Lett.* **35** 1652
[4] Defrain A 1977 *J. Chim. Phys. Phys.-Chim. Biol.* **74** 851
[5] Pochon S, MacDonald K F, Knize R J and Zheludev N I 2004 *Phys. Rev. Lett.* **92** 145702
[6] Soares B F, MacDonald K F, Fedotov V A and Zheludev N I 2005 *Nano Lett.* **5** 2104
[7] Perepezko J H 1984 *Mater. Sci. Eng.* **65** 125
[8] Parravicini G B, Stella A, Ghigna P, Spinolo G, Migliori A, d'Acapito F and Kofman R 2006 *Appl. Phys. Lett.* **89** 033123
[9] Poloni R, De Panfilis S, Di Cicco A, Pratesi G, Principi E, Trapananti A and Filipponi A 2005 *Phys. Rev.* B **71** 184111
[10] Charnaya E V, Tien C, Lin K J and Kumzerov Yu A 1998 *J. Phys.: Condens. Matter* **10** 7273
[11] Charnaya E V, Tien C, Lin K J and Kumzerov Yu A 1998 *Phys. Rev.* B **58** 11089
[12] He H, Fei G T, Cui P, Zheng K, Liang L M, Li Y and Zhang L D 2005 *Phys. Rev.* B **72** 073310
[13] He H, Chen X M, Fei G T, Cui P, Zheng K, Shui J P and Zhang R L 2007 *Phys. Lett.* A **369** 107
[14] Tien C, Wur C S, Lin K J, Hwang J S, Charnaya E V and Kumzerov Yu A 1996 *Phys. Rev.* B **54** 11880
[15] Tien C, Charnaya E V, Wang W Y, Kumzerov Yu A and Michel D 2006 *Phys. Rev.* B **74** 024116
[16] Teske D and Drumheller J E 1999 *J. Phys.: Condens. Matter* **11** 4935
[17] Konrad H, Weissmüller J, Birringer R, Karmonik C and Gleiter H 1998 *Phys. Rev.* B **58** 2142
[18] Liu Z W, Bando Y, Mitome M and Zhan J H 2004 *Phys. Rev. Lett.* **93** 095504
[19] Di Cicco A, Fusari S and Stizza S 1999 *Phil. Mag.* B **79** 2113
[20] Di Cicco A 1998 *Phys. Rev. Lett.* **81** 2942
[21] Bosio L, Defrain A and Epelboin I 1966 *J. Physique* **27** 61